



A Journal of the Gesellschaft Deutscher Chemiker

Angewandte Chemie

GDCh

International Edition

www.angewandte.org

Accepted Article

Title: Atomically dispersed Ru species inside MOFs combining high activity of atomic sites and molecular sieving effect of MOFs

Authors: Yadong Li, Shufang Ji, Yuanjun Chen, Shu Zhao, Wenxing Chen, Lijun Shi, Yu Wang, Juncai Dong, Zhi Li, Fuwei Li, Chen Chen, Qing Peng, Jun Li, and Dingsheng Wang

This manuscript has been accepted after peer review and appears as an Accepted Article online prior to editing, proofing, and formal publication of the final Version of Record (VoR). This work is currently citable by using the Digital Object Identifier (DOI) given below. The VoR will be published online in Early View as soon as possible and may be different to this Accepted Article as a result of editing. Readers should obtain the VoR from the journal website shown below when it is published to ensure accuracy of information. The authors are responsible for the content of this Accepted Article.

To be cited as: *Angew. Chem. Int. Ed.* 10.1002/anie.201814182
Angew. Chem. 10.1002/ange.201814182

Link to VoR: <http://dx.doi.org/10.1002/anie.201814182>
<http://dx.doi.org/10.1002/ange.201814182>

COMMUNICATION

Atomically dispersed Ru species inside MOFs combining high activity of atomic sites and molecular sieving effect of MOFs

Shufang Ji, Yuanjun Chen, Shu Zhao, Wenxing Chen, Lijun Shi, Yu Wang, Juncai Dong, Zhi Li, Fuwei Li, Chen Chen, Qing Peng, Jun Li, Dingsheng Wang*, Yadong Li*

Abstract: Incorporating atomically dispersed metal species into functionalized metal-organic frameworks (MOFs) can integrate their respective merits to have important applications in catalysis. Here we report a cage-controlled encapsulation and reduction strategy to fabricate single Ru atoms and triatomic Ru₃ clusters anchored on ZIF-8 (Ru₁@ZIF-8, Ru₃@ZIF-8). The highly efficient and selective catalysis for semi-hydrogenation of alkyne is observed. The excellent activity derives from high atom-efficiency of atomically dispersed Ru active sites and hydrogen enrichment by ZIF-8 shell. Meanwhile, ZIF-8 shell serves as a novel “molecular sieve” for olefins to achieve the absolute regioselectivity of catalyzing terminal alkynes but not internal alkynes. Moreover, the size-dependent performance between Ru₃@ZIF-8 and Ru₁@ZIF-8 is detected in experiment and understood by quantum-chemical calculations, demonstrating a new and promising approach to optimize catalysts by precisely controlling the number of atoms.

Developing heterogeneous catalysts with high activity and selectivity has become a focus in catalysis research^[1]. Metal-organic frameworks (MOFs) are known as a new class of porous crystalline materials^[2], whose high porosity facilitates accessibility of active species and boosts efficiency by enriching gas molecules^[3]. In addition, the regularity of pore sizes render molecular sieving function, which can enhance selectivity by regulating the transport and diffusion of substrates^[3b,4]. Incorporating metal nanoparticles (MNPs) into metal-organic frameworks (MOFs) can inherit the above advantages of MOFs and facilitate catalysis^[5]. However, these MNPs/MOFs composites are confronted with some shortages that limit their further enhancement on catalytic performance. Most synthetic routes to

MNPs/MOFs composites undergo a high-temperature reduction to transform metal precursors into nanoparticles, which is hard to control the dispersion property and uniformity^[6]. Such structural heterogeneity becomes a key obstacle to improve catalytic selectivity because substrates may adsorb on different structural surfaces and undergo different reaction pathways, leading to generation of side products. Catalytic reactions take place primarily on the surface of metal nanoparticles, while inner atoms usually do not participate^[7]. Thus, metal nanoparticles suffer from low metal atom-utilization efficiency and significant decline in the number of exposed active sites compared with single atoms and clusters.

As a bridge between homogeneous and heterogeneous catalysis, atomically dispersed catalysts integrate their advantages of homogenized active sites and easy recovery, which have delivered extraordinary activity in a variety of reactions^[8]. And the nature of uniform sites is expected to enhance selectivity owing to similar spatial and electronic interaction with substrates^[9]. Moreover, well-defined structure and coordination environment are conducive to identification of active sites, which facilitates studies of structure-performance relationship at atomic level^[10]. Therefore, developing an effective strategy to form uniform atomically dispersed active sites, and simultaneously make them be incorporated into functionalized MOFs is highly desirable, which can combine the merits of atomic sites and MOFs to synergistically enhance catalytic performance.

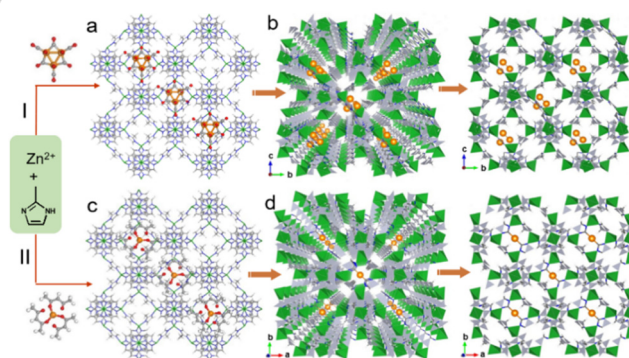


Figure 1. Schematic preparation process of (a,b) Ru₃@ZIF-8 and (c,d) Ru₁@ZIF-8 catalyst.

Herein, we construct single Ru atoms and triatomic Ru₃ clusters confined in functionalized ZIF-8 via a cage-controlled encapsulation and reduction strategy (Ru₁@ZIF-8, Ru₃@ZIF-8). For semi-hydrogenation of phenylacetylene, Ru₃@ZIF-8 exhibit excellent activity with the turnover frequency (TOF) of 360 h⁻¹, absolute regioselectivity of catalyzing terminal alkynes (but not internal alkynes) and outstanding chemoselectivity of 97% for

[*] S. Ji^[†], Y. Chen^[†], Dr. W. Chen, Dr. Z. Li, Prof. C. Chen, Prof. Q. Peng, Prof. J. Li, Prof. D. Wang, Prof. Y. Li
Department of Chemistry, Tsinghua University, Beijing 100084
China
E-mail: wangdingsheng@mail.tsinghua.edu.cn
ydlj@mail.tsinghua.edu.cn

Dr. S. Zhao^[†]

Beijing Guyue New Materials Research Institute, Beijing University of Technology, Beijing 100124, China

L. Shi, Prof. F. Li

State Key Laboratory for Oxo Synthesis and Selective Oxidation, Suzhou Research Institute of LICP, Lanzhou Institute of Chemical Physics (LICP), Chinese Academy of Sciences, Lanzhou 730000, China

Dr. Y. Wang

Shanghai Synchrotron Radiation Facilities, Shanghai Institute of Applied Physics, Chinese Academy of Sciences, Shanghai 201204, China

Dr. J. Dong

Beijing Synchrotron Radiation Facility, Institute of High Energy Physics, Chinese Academy of Sciences, Beijing, China

[†] These authors contributed equally to this work.

Supporting information for this article is given via a link at the end of the document.

COMMUNICATION

styrene. The highly efficient and selective catalysis are ascribed to atomically dispersed Ru sites and molecular sieving effect of MOFs. Moreover, the size-dependent performance is evidently detected, with Ru₃@ZIF-8 exhibiting better activity and selectivity than Ru₁@ZIF-8. We further carried out density functional theory (DFT) calculations to evaluate the difference of structural properties and the reaction mechanism between Ru₃@ZIF-8 and Ru₁@ZIF-8 to better understand drastically different properties.

To achieve our design goal of atomically dispersed metal species and MOFs composites, we used MOFs as hosts to *in-situ* encapsulate and separate preselected precursors, followed by thermal treatment for removing the ligands. The preparation process is illustrated in Figure 1. The preselected precursor Ru₃(CO)₁₂ was in situ encapsulated during the crystallization of ZIF-8 (Ru₃(CO)₁₂@ZIF-8, Figure 1a and Figure S1a to S1e). The synthesis of Ru(acac)₃@ZIF-8 is the same as the above procedure expect that Ru₃(CO)₁₂ is replaced by Ru(acac)₃ (Figure 1c and S1f). The combination of measurements was performed (Figure S2 to S7) to confirm that Ru₃(CO)₁₂ and Ru(acac)₃ were respectively encapsulated within ZIF-8. Then, Ru₃(CO)₁₂@ZIF-8 and Ru(acac)₃@ZIF-8 underwent thermal reduction treatment to form Ru₃ clusters and Ru₁ single atoms stabilized by the framework of ZIF-8 (Figure 1b,d).

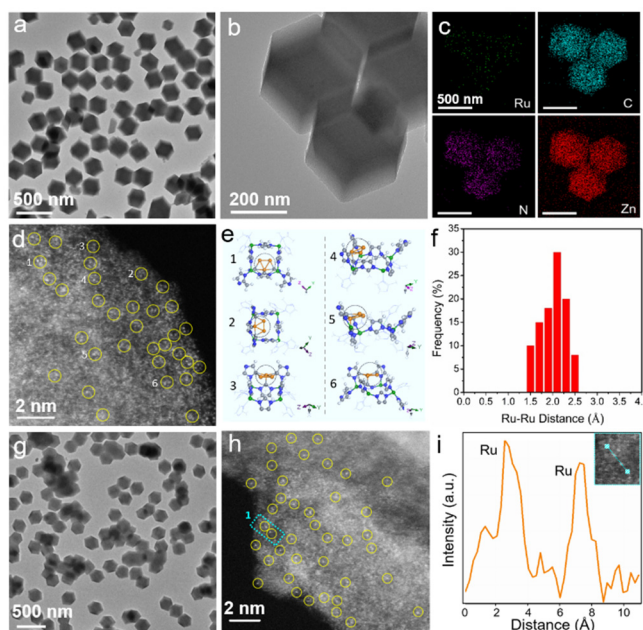


Figure 2. (a) TEM, (b) enlarged TEM, (c) EDS maps, (d) AC HAADF-STEM images of Ru₃@ZIF-8, (e) Illustrations of Ru₃ clusters from top and side view. (f) Statistical Ru–Ru distance in the observed Ru₃ clusters. (g) TEM and (h) AC HAADF-STEM images of Ru₁@ZIF-8. (i) Intensity file of Ru₁@ZIF-8 in the cyan dotted rectangle area of Figure 1h.

Transmission electron microscopy (TEM) images demonstrate that Ru₃@ZIF-8 and Ru₁@ZIF-8 display a rhombic dodecahedron morphology (Figures 2a, b and g). The XRD patterns of Ru₃@ZIF-8 and Ru₁@ZIF-8 exhibit characteristic peaks of ZIF-8, indicating the crystallinity of ZIF-8 is not destroyed

(Figure S2), consistent with FTIR results (Figure S3 and S4). And energy-dispersive X-ray spectroscopy (EDS) analysis confirm that Ru, C, N and Zn elements were uniformly distributed (Figure 2c and S8). To directly observe the dispersion of Ru at atomic scale, aberration-corrected HAADF-STEM (AC HAADF-STEM) was carried out. Due to the Z-contrast, brighter dots (identified as Ru atoms) can be distinguished from ZIF-8 matrix^[11]. A group of three brighter dots marked by yellow circles is in agreement with triangular Ru₃ clusters (Figure 2d), while the observation of two adjacent bright dots coincides with Ru₃ clusters that are not over against the projection direction for several possible structures by DFT simulation (Figure 2e and area 1 to area 6 in Figure 2d). From different areas in AC HAADF-STEM images (Figure 2d and S9), statistical analysis of Ru–Ru distance from more than 100 pairs of neighboring Ru atoms were performed, revealing Ru–Ru distance at 2.2±0.3 Å, consistent with Ru–Ru bond lengths of Ru₃ clusters (Figure 2f). For Ru₁@ZIF-8, as observed by isolated brighter dots and the intensity profiles (Figure 2h,i), isolated Ru atoms are uniformly dispersed in Ru₁@ZIF-8.

To gain local structure of Ru₃@ZIF-8 and Ru₁@ZIF-8, X-ray absorption near-edge structure (XANES) and extended X-ray absorption fine structure (EXAFS) were performed. The energy absorption threshold values of Ru₃@ZIF-8 and Ru₁@ZIF-8 are between those of RuO₂ and Ru foil (Figure 3a), suggesting Ru₃ clusters and Ru₁ single atoms carry partially positive charge. The Fourier transform (FT) of EXAFS spectra are shown in Figure 3b. For Ru₁@ZIF-8, only one obvious Ru–C scattering peak around ~1.5 Å is detected. And no scattering peaks from Ru–Ru coordination is observed, revealing the sole presence of isolated Ru atoms. Whereas, at the FT curve of Ru₃@ZIF-8, besides a strong peak at ~1.5 Å from Ru–C contribution, another higher shell peak located at ~2.4 Å are detected, indicating the presence of Ru–Ru contribution derived from Ru₃ clusters.

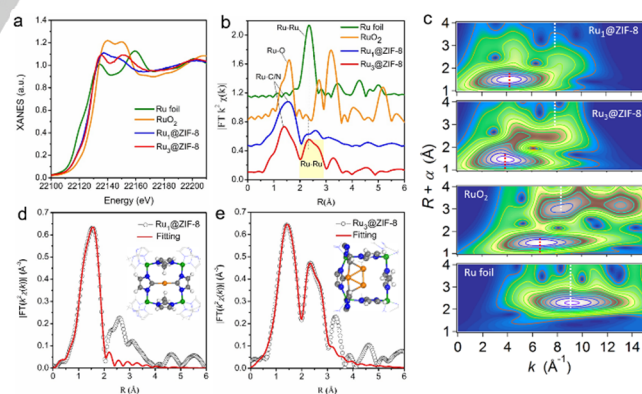


Figure 3. (a) XANES, (b) EXAFS, (c) WT of Ru₁@ZIF-8, Ru₃@ZIF-8, RuO₂ and Ru foil, respectively. Corresponding EXAFS *R* space fitting curve of (d) Ru₁@ZIF-8 and (e) Ru₃@ZIF-8, respectively. Inset: Simulations models of Ru₁@ZIF-8 and Ru₃@ZIF-8, respectively.

To further reinforce atomic structure of Ru₃@ZIF-8 and Ru₁@ZIF-8, we carried out Wavelet transform (WT) analysis, which can provide powerful resolution in both *k* and *R* spaces^[12].

COMMUNICATION

Figure 3c shows that WT plot of $\text{Ru}_1@ZIF-8$ displays only one intensity maximum near $\sim 4.0 \text{ \AA}^{-1}$ from Ru-C backscattering contributions. Compared with Ru foil, no other maximum at around 8.0 \AA^{-1} is detected in the higher shell peak, suggesting that the sole dispersion of single-atom Ru. For $\text{Ru}_3@ZIF-8$, two intensity maximum at $\sim 4.0 \text{ \AA}^{-1}$ and $\sim 8.0 \text{ \AA}^{-1}$ are observed for Ru species. 4.0 \AA^{-1} of intensity maximum is assigned to Ru-C path, implying Ru-C contribution of the first nearest-neighbor coordination shell. Whereas the other obvious intensity maximum at near 8.0 \AA^{-1} in the higher coordination shell can be attributed to the presence of Ru-Ru scattering contribution. All the findings demonstrate that Ru clusters are atomically dispersed in $\text{Ru}_3@ZIF-8$. Quantitative EXAFS curve fittings were performed to extract the structural parameters in **Table S1** and the fitting results are summarized in **Figure 3d, e** and **Figure S10 to S12**. The most stable structures of $\text{Ru}_1@ZIF-8$ and $\text{Ru}_3@ZIF-8$ samples are further verified by first-principles calculations (insets of **Figure 3d** and **3e**, **Table S2** and **S3**).

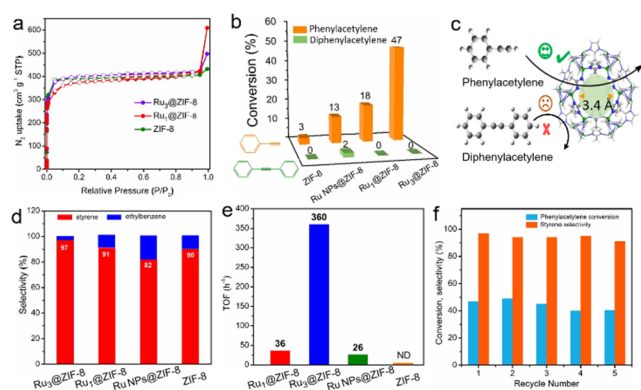


Figure 4. Studies of catalytic properties for $\text{Ru}_3@ZIF-8$ and $\text{Ru}_1@ZIF-8$ catalysts. (a) Nitrogen-sorption isotherms, (b) conversion, (c) molecular sieving size-selectivity sketch of phenylacetylene and diphenylacetylene, (d) selectivity and (e) TOFs for hydrogenation of phenylacetylene over $\text{Ru}_3@ZIF-8$, $\text{Ru}_1@ZIF-8$ and references. (f) Catalytic performance of $\text{Ru}_3@ZIF-8$ for several recycles of repeated reactions.

From the N_2 adsorption and desorption isotherms (**Figure 4a**), the N_2 sharp uptake indicates a standard type I isotherm, implying the existence of microporosity for $\text{Ru}_3@ZIF-8$ and $\text{Ru}_1@ZIF-8$. **Figure S13** demonstrates the incorporation of Ru_3 clusters and Ru_1 single atoms does not alter the pore-size distribution of ZIF-8.

Integrating unique properties of atomically dispersed species and versatile functionalities of MOFs, $\text{Ru}_3@ZIF-8$ and $\text{Ru}_1@ZIF-8$ composites have great potential applications in catalysis. Hydrogenation of phenylacetylene and diphenylacetylene were thus chosen as model reactions. As shown in **Figure 4b**, $\text{Ru}_3@ZIF-8$ and $\text{Ru}_1@ZIF-8$ both exhibit significant conversion of phenylacetylene (47% for $\text{Ru}_3@ZIF-8$ and 18% for $\text{Ru}_1@ZIF-8$). Negligible activity of $\text{Ru}_3@ZIF-8$ and $\text{Ru}_1@ZIF-8$ are detected in catalyzing hydrogenation of diphenylacetylene. The obviously different conversion for alkynes demonstrated the selective catalysis is successfully achieved by molecular sieving effect of ZIF-8 shell. Owing to the steric effect of restriction, compared with

carbon-carbon triple bonds ($\text{C}\equiv\text{C}$) at the end of phenyl ethyne, intramolecular $\text{C}\equiv\text{C}$ of diphenylacetylene cannot contact encapsulated Ru active species, resulting in absolute regioselectivity (**Figure 4c**). To further confirm the regioselectivity of catalyzing terminal unsaturated hydrocarbon but not internal unsaturated hydrocarbon, other substrate molecules are chosen and the catalytic results are summarized in **Table S4**. In addition, the excellent styrene selectivity is 97% for $\text{Ru}_3@ZIF-8$ and 91% for $\text{Ru}_1@ZIF-8$, implying a high chemoselectivity (**Figure 4d**). For comparison, Ru nanoparticles encapsulated in ZIF-8 (marked Ru NPs@ZIF-8) were prepared and fully characterized (**Figure S14** and **15**), which exhibits lower conversion (13%) and poorer selectivity (82%). And few activity is observed for pure ZIF-8. Furthermore, the TOF of $\text{Ru}_3@ZIF-8$ achieves as high as 360 h^{-1} , which is 10 times and 13.8 times of $\text{Ru}_1@ZIF-8$ (36 h^{-1}) and Ru NPs@ZIF-8 (26 h^{-1}) (**Figure 4e**). The enhanced performance is attributed to atomically dispersed Ru_3 clusters and ZIF-8 shell as well-confined nanoreactors for hydrogen enrichment. To assess the recyclability of $\text{Ru}_3@ZIF-8$, five consecutive runs were performed. Similar conversion and selectivity are detected compared with fresh catalyst, indicating excellent recyclability (**Figure 4f**). Moreover, the spent catalyst were fully characterized, which clearly reveals atomic dispersion of Ru and framework of ZIF-8 are well preserved (**Figure S16** and **S17**).

It is worth noting that $\text{Ru}_3@ZIF-8$ and $\text{Ru}_1@ZIF-8$ exhibit different catalytic performance for the selective hydrogenation of phenylacetylene, with $\text{Ru}_3@ZIF-8$ possessing higher activity and selectivity. This observed result provides a successful paradigm for demonstrating size-dependent effect between single-atom and multi-atom catalysts. To further investigate this size-dependent effect, we selected acetylene (the simplest alkynes molecule) as a model substrate. The molecular size of acetylene (2.5 \AA) is smaller than the pore aperture size of ZIF-8 (3.4 \AA)^[13], acetylene can enrich in and diffuse through the pore apertures of ZIF-8 without obstacle. **Figure 5a** shows that activity of $\text{Ru}_3@ZIF-8$ ($603.6 \text{ molC}_2\text{H}_2 \text{ mol}^{\text{noble metal}^{-1}} \text{ h}^{-1}$) is higher than that of $\text{Ru}_1@ZIF-8$ ($12.5 \text{ molC}_2\text{H}_2 \text{ mol}^{\text{noble metal}^{-1}} \text{ h}^{-1}$). And $\text{Ru}_3@ZIF-8$ exhibits better ethylene selectivity of $\sim 84\%$ than $\text{Ru}_1@ZIF-8$ (**Figure 5b**).

To better understand drastically different properties between $\text{Ru}_3@ZIF-8$ and $\text{Ru}_1@ZIF-8$, DFT calculations were performed. The energy profiles containing the entropic effects from gas phase acetylene and hydrogen to gas phase ethane on $\text{Ru}_1@ZIF-8$ and $\text{Ru}_3@ZIF-8$ are shown in **Figure 5c**. The computational details are in the Supporting Information (**Table S5-S7** and **Figure S18-23**). On $\text{Ru}_3@ZIF-8$, the first hydrogenation step is found to have the lowest activation barrier (**TS1**, 0.39 eV) in the whole pathway and exothermic by 0.47 eV . The next two steps have higher barriers of 0.93 eV (**TS2**) and 0.85 eV (**TS3**), and the reactions are exothermic by 0.40 eV and 0.04 eV , respectively. Desorption energy of C_2H_4 at 500 K is 0.57 eV , smaller than its further hydrogenation barrier (0.85 eV). More importantly, the transition-state energy of C_2H_4 hydrogenation (**TS3**) is above the energy of gas-phase ethylene (**Figure 5c**), which suggests that the ethylene prefers desorption to further hydrogenation in the following process.

On $\text{Ru}_1@ZIF-8$, heterolysis of H_2 has a low barrier of 0.23 eV , and exothermic by 0.66 eV (**Figure S23**). After dissociation, one

COMMUNICATION

of the hydrogen adsorbed on Ru atom and the other one bonds to the carbon atom in ZIF-8. The hydrogenation of C_2H_2 to C_2H_3 is most kinetically feasible among the whole hydrogenation processes, with a barrier of 0.23 eV (**TS1**). Then, H migrates from ZIF-8 to the single Ru site with a high barrier of 1.35 eV (**TS-H1**), and strongly endothermic by 0.88 eV. The next step ($C_2H_3 + H \rightarrow C_2H_4$) has a barrier of 1.11 eV (**TS2**), and highly exothermic by 0.70 eV. The further hydrogenation of C_2H_4 to C_2H_5 has barrier of 1.01 eV (**TS3**), which is lower than the desorption energy of C_2H_4 (1.33 eV) and much lower than the energy of gas-phase ethylene at 500 K (**Figure 5c**). Thus, C_2H_4 will be further hydrogenated to undesirable ethane rather than desorbed directly. For the whole hydrogenation pathway, the effective barrier on $Ru_1@ZIF-8$ is much higher than that on $Ru_3@ZIF-8$ (2.17 vs. 1.43 eV), indicating that the $Ru_3@ZIF-8$ catalyst is more active for the semi-hydrogenation of acetylene than $Ru_1@ZIF-8$. A high selective catalyst should have a low desorption energy and a high hydrogenation barrier of ethylene. So the difference (ΔE) between the hydrogenation barrier and the desorption energy of C_2H_4 is calculated to estimate the selectivity (**Table S8**)^[14]. We find that $Ru_3@ZIF-8$ has higher ΔE (0.28 eV) than $Ru_1@ZIF-8$ (-0.32 eV), suggesting the $Ru_3@ZIF-8$ is more selective to semi-hydrogenation of acetylene.

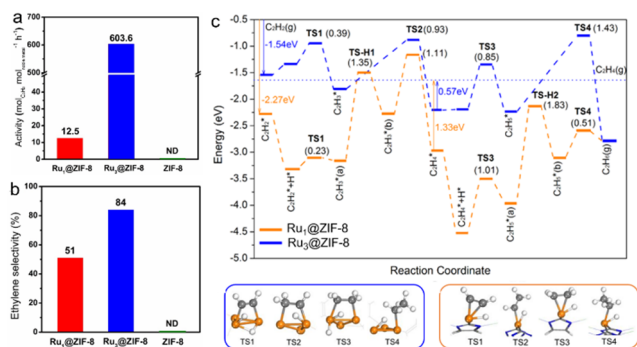


Figure 5. Size-dependent effect of uniform controlled ruthenium species for hydrogenation reaction. (a) Reaction activity and (b) ethylene selectivity in selective hydrogenation of acetylene on $Ru_1@ZIF-8$, $Ru_3@ZIF-8$ and ZIF-8. (c) Step-by-step hydrogenation mechanism of acetylene to ethane on the $Ru_1@ZIF-8$ and $Ru_3@ZIF-8$. Structures of transition states of C_2H_2 hydrogenation on $Ru_3@ZIF-8$ (blue line) and $Ru_1@ZIF-8$ (yellow line) (Ru: orange, C: gray, H: white).

In summary, we develop an effective strategy to construct ideal composites by combining the advantages of atomically dispersed Ru species and functionalized MOF, which synergistically facilitate catalysis. In this work, $Ru_3@ZIF-8$ and $Ru_1@ZIF-8$ demonstrate the following advantages: (1) The spatial separation of Ru single atom and triatomic Ru_3 cluster is precontrolled by cages of ZIF-8 to prevent active species from migration and agglomeration for excellent stability and recyclability; (2) atomic dispersion of active Ru species with maximum atom efficiency and H_2 enrichment by porous structure of ZIF-8 is beneficial for enhanced activity; (3) molecular sieve effect of MOF enables selection of substrates to exhibit absolute regioselectivity of catalyzing terminal alkynes but not internal

alkynes; and (4) outstanding chemoselectivity of semi-hydrogenation with hydrogenating alkynes to alkenes is achieved by intrinsic nature of atomically dispersed Ru species. Moreover, the size-dependent performance between $Ru_3@ZIF-8$ and $Ru_1@ZIF-8$ is observed in experiment and understood by DFT studies, which provides a concrete paradigm to reveal that tunable catalytic performance can be achieved by precious control on the number of atoms. These findings present a promising inkling to design and optimize catalysts by combining high performance of atomic sites and molecular sieving effect of MOFs. The new catalysts based on Ru_1 and Ru_3 cluster reveal the promise of utilizing well-defined, controllable single-atom and single-cluster active centers in catalytic design for complicated chemical reactions.^[15]

Acknowledgements

This work was supported by China Ministry of Science and Technology under Contract of 2016YFA (0202801), the National Natural Science Foundation of China (21521091, 21390393, U1463202, 21471089, 21671117, 91645203, 21590792) and the Beijing Natural Science Foundation (2184097). We thank Shanghai Light Source for use of the instruments. The calculations were performed using supercomputers at Tsinghua National Laboratory for Information Science and Technology and the Supercomputer Center of the Computer Network Information Center at the Chinese Academy of Sciences.

Keywords: single atom • cluster • MOFs • composites • catalyst

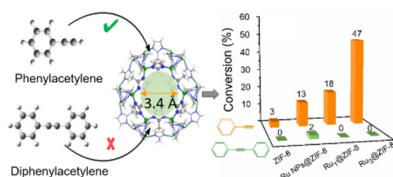
- [1] a) E. Gross, G. A. Somorjai, *Top. Catal.* **2013**, *56*, 1049-1058; b) R. Noyori, *Nat. Chem.* **2009**, *1*, 5-6; c) K. Na, K. M. Choi, O. M. Yaghi, G. A. Somorjai, *Nano. Lett.* **2014**, *14*, 5979-5983; d) G. Chen, C. Xu, X. Huang, J. Ye, L. Gu, G. Li, Z. Tang, B. Wu, H. Yang, Z. Zhao, Z. Zhou, G. Fu, N. Zheng, *Nat. Mater.* **2016**, *15*, 564-569.
- [2] a) H. Furukawa, K. E. Cordova, M. O'Keeffe, O. M. Yaghi, *Science* **2013**, *341*, 1230444; b) A. J. Howarth, Y. Liu, P. Li, Z. Li, T. C. Wang, J. T. Hupp, O. K. Farha, *Nat. Rev. Mater.* **2016**, *1*, 15018.
- [3] a) G. Li, H. Kobayashi, J. M. Taylor, R. Ikeda, Y. Kubota, K. Kato, M. Takata, T. Yamamoto, S. Toh, S. Matsumura, H. Kitagawa, *Nat. Mater.* **2014**, *13*, 802-806; b) M. Zhao, K. Yuan, Y. Wang, G. Li, J. Guo, L. Gu, W. Hu, H. Zhao, Z. Tang, *Nature* **2016**, *539*, 76-80.
- [4] a) G. Lu, S. Li, Z. Guo, O. K. Farha, B. G. Hauser, X. Qi, Y. Wang, X. Wang, S. Han, X. Liu, J. S. DuChene, H. Zhang, Q. Zhang, X. Chen, J. Ma, S. C. Loo, W. D. Wei, Y. Yang, J. T. Hupp, F. Huo, *Nat. Chem.* **2012**, *4*, 310-316; b) Z. Li, R. Yu, J. Huang, Y. Shi, D. Zhang, X. Zhong, D. Wang, Y. Wu, Y. Li, *Nat. Commun.* **2015**, *6*, 8248.
- [5] a) L. Chen, R. Luque, Y. Li, *Chem. Soc. Rev.* **2017**, *46*, 4614-4630; b) Q. Yang, Q. Xu, H. L. Jiang, *Chem. Soc. Rev.* **2017**, *46*, 4774-4808.
- [6] a) Z. Guo, C. Xiao, R. V. Maligal-Ganesh, L. Zhou, T. W. Goh, X. Li, D. Tesfagaber, A. Thiel, W. Huang, *ACS Catal.* **2014**, *4*, 1340-1348.; b) Q. L. Zhu, J. Li, Q. Xu, *J. Am. Chem. Soc.* **2013**, *135*, 10210-10213.
- [7] a) N. Ta, J. Liu, S. Chenna, P. A. Crozier, Y. Li, A. Chen, W. Shen, *J. Am. Chem. Soc.* **2012**, *134*, 20585-20588; b) J. H. K. Pfisterer, Y. Liang, O. Schneider, A. S. Bandarenka, *Nature* **2017**, *549*, 74.
- [8] a) B. Qiao, A. Wang, X. Yang, L. F. Allard, Z. Jiang, Y. Cui, J. Liu, J. Li, T. Zhang, *Nat. Chem.* **2011**, *3*, 634-641; b) M. Hu, J. Zhang, W. Zhu, Z. Chen, X. Gao, X. Du, J. Wan, K. Zhou, C. Chen, Y. Li, *Nano Res.* **2018**, *11*, 905-912.; c) H. Yang, C. Wang, F. Hu, Y. Zhang, H. Lu, Q. Wang, *Sci. China Mater.* **2017**, *60*, 1-8; d) X. Qiu, J. Chen, X. Zou, R. Fang, L. Chen,

COMMUNICATION

- Z. Chen, K. Shen, Y. Li, *Chem. Sci.* **2018**, (DOI: 10.1039/C8SC03549K).
- [9] a) L. Wang, W. Zhang, S. Wang, Z. Gao, Z. Luo, X. Wang, R. Zeng, A. Li, H. Li, M. Wang, X. Zheng, J. Zhu, W. Zhang, C. Ma, R. Si, J. Zeng, *Nat. Commun.* **2016**, 7, 14036; b) X. Guo, G. Fang, G. Li, H. Ma, H. Fan, L. Yu, C. Ma, X. Wu, D. Deng, M. Wei, D. Tan, R. Si, S. Zhang, J. Li, L. Sun, Z. Tang, X. Pan, X. Bao, *Science* **2014**, 344, 616-619.
- [10] a) Y. Chen, S. Ji, Y. Wang, J. Dong, W. Chen, Z. Li, R. Shen, L. Zheng, Z. Zhuang, D. Wang, Y. Li, *Angew. Chem. Int. Ed.* **2017**, 56, 6937-6941; b) S. Yang, J. Kim, Y. J. Tak, A. Soon, H. Lee, *Angew. Chem. Int. Ed.* **2016**, 55, 2058-2062; c) Y. Chen, S. Ji, C. Chen, Q. Peng, D. Wang, Y. Li, *Joule* **2018**, 2, 1242-1264.
- [11] V. Ortalan, A. Uzun, B. C. Gates, N. D. Browning, *Nat. Nanotechnol.* **2010**, 5, 843-847.
- [12] H. Funke, A. C. Scheinost, M. Chukalina, *Phys. Rev. B* **2005**, 71, 094110.
- [13] D. Fairen-Jimenez, S. A. Moggach, M. T. Wharmby, P. A. Wright, S. Parsons, T. Duren, *J. Am. Chem. Soc.* **2011**, 133, 8900-8902.
- [14] B. Yang, R. Burch, C. Hardacre, G. Headdock, Hu, P. *ACS Cat.* **2012**, 2, 1027-1032.
- [15] a) S. Zhang, L. Nguyen, J.-X. Liang, J. Shan, J. Liu, A. I. Frenkel, A. Pattolla, W. Huang, J. Li, F. Tao, *Nat. Commun.* **2015**, 6, 7938; b) X.-L. Ma, J.-C. Liu, H. Xiao, J. Li, *J. Am. Chem. Soc.* **2018**, 140, 46-49; c) J.-C. Liu, X.-L. Ma, Y. Li, Y.-G. Wang, H. Xiao, J. Li, *Nat. Commun.* **2018**, 9, 1610.

COMMUNICATION

COMMUNICATION



Single Ru atoms and triatomic Ru₃ clusters confined in functionalized ZIF-8 as composites catalysts integrate the advantages of atomically dispersed Ru species and microporous MOF structure, which synergistically facilitate highly efficient and selective catalysis for semi-hydrogenation of alkyne and exhibit the molecular sieve effect. The experiments and theoretical calculations further reveal the size-dependent performance between Ru₃@ZIF-8 and Ru₁@ZIF-8 catalysts.

Shufang Ji, Yuanjun Chen, Shu Zhao, Wenxing Chen, Lijun Shi, Yu Wang, Juncai Dong, Zhi Li, Fuwei Li, Chen Chen, Qing Peng, Jun Li, Dingsheng Wang*, Yadong Li*

Page No. – Page No.

Atomically dispersed Ru species inside MOFs combining high activity of atomic sites and molecular sieving effect of MOFs

Accepted Manuscript